2024 IEEE International Conference on Robotics and Automation (ICRA 2024)
May 13-17, 2024. Yokohama, Japan

Self-Reconfigurable Robots for Collaborative Discrete Lattice Assembly

Miana Smith[1], Amira Abdel-Rahman[1], and Neil Gershenfeld[1]

Abstract— **We present a robotic system for the assembly of 3D discrete lattice structures in which the robots are able to self-reproduce, such that the assembly system may scale its own parallelization. Robots and structures are made from a set of compatible building blocks, or voxels, which can be assembled and reassembled into more complex structures. Robotic modules are made by combining actuators with a functional voxel, which routes electrical power and signals. Robotic modules then assemble into reconfigurable robots via a reversible solder joint. The robot assembles higher performance structures using a set of construction voxels, which do not contain electrical features. This paper describes the design, development, and evaluation of this assembly system, including the robotic hardware, lattice material, and planning and controls methods. We demonstrate the system through a set of fundamental assembly tasks: the robot assembling another robot, and the two robots collaborating to assemble a small structure.**

I. INTRODUCTION

The autonomous assembly of large, high performance structures remains limited by the size and complexity of the necessary machines. As the size of the machine gets larger, the demands on the relative precision of the machine also get larger; the machine must travel larger distances while maintaining a low error threshold in material placement. Assembly-based approaches to building large structures using discrete elements can address this scaling problem by introducing error-correcting features into the discrete feedstock— the precision of the assembled material corrects for imprecision in the assembler [1]. Mobile assembly robots can be used to decouple assembler size from the size of the final structure, enabling the construction of arbitrarily sized structures [2]. This style of robotic assembly has been demonstrated with both highly complex robotic systems, such as with aerial drones [3] or arms mounted on moving bases [4], as well as with relatively simple robots, by co-designing the assembled material with the robot such that the underlying material corrects for errors in the robotic system [2]. This style of "relative robot" assembly often uses a robot which directly locomotes over the assembled structure, such as in [2], [5], [6], or which uses a combination of robots to deliver and place new material, such as in [7] or [8].

However, it is inefficient to build large structures if a robot must continuously traverse the entire structure to pick and place single new material units. To improve the efficiency, we can increase the parallelization of the assembly system by using a modular robot, enabling a robot to assemble either more of the target structure, more robots, or larger robots that are able to manipulate more material at once. In this way, the swarm can scale itself to the construction task at hand. In simulation, [9] demonstrates that taking this self-replicating hierarchical approach can optimize the efficiency of constructing large structures.

The goal of this work is to provide a functional hardware basis for realizing this style of robotic assembly system. We introduce a hardware basis for realizing the self-reproducing robotic assembly system described in [9], addressing physical limitations of the robots used in [2] and [9] that prevented them from assembling load bearing systems or self-replicating, respectively. In our system, as in [9], the assembly robot itself is composed of modules compatible with the material it assembles (see Fig. 1), and we have iterated both these modules and the building material system (or voxels) so that they form structural connections. We demonstrate this system through the assembly of small-scale structural voxel primitives and through the robotic assembly of a second robot that can then assist in further voxel assembly.

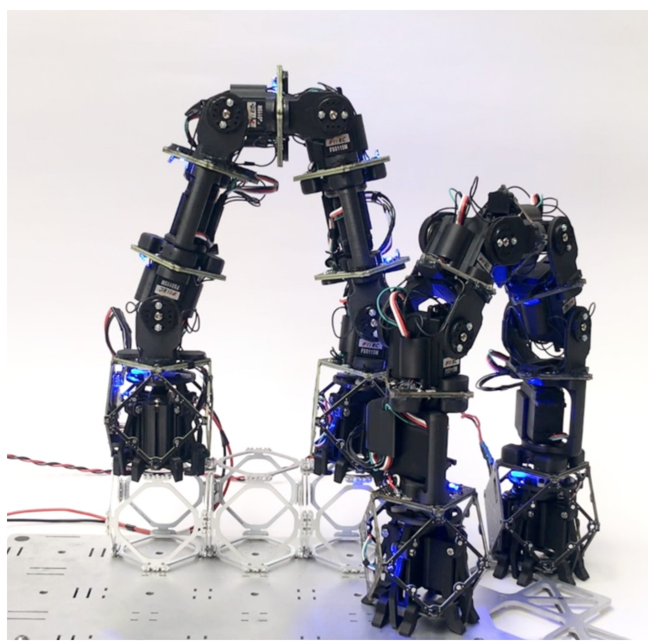

Fig. 1. Two robotic assemblers standing on a build plate that provides a stable starting point for the assembly of larger voxel structures. The robot on the right was assembled by the robot on the left.

This work in part appears in the thesis available here: https://hdl.handle.net/1721.1/152015

[1]Authors are with the Center for Bits and Atoms, Massachusetts Institute of Technology, Cambridge, MA 02139 USA (emails: miana@mit.edu, amira.abdel-rahman@cba.mit.edu, gersh@cba.mit.edu). Corresponding author: miana@mit.edu

II. BACKGROUND

Cellular materials or architected materials represent a solution for distributing material efficiently and effectively in space. In engineering applications, these materials are often used in systems that need to be lightweight without sacrificing mechanical performance. Cellular materials span a range of sizes and purposes— at the very large scale, we might recognize a truss bridge as a cellular material assembly, and at the other end of the size scale are micro-lattices with features on the order of 100s of microns [10]. Much of the current research in producing this type of structure is focused on materials with very small features— lattice pitches on the size scales of 100s to 1000s of microns, which then form material samples on the size scale of centimeters [11] [10] [12]. The manufacturing techniques required for producing material at this scale, such as two-photon lithography 3D printing, would be difficult to scale up to sizes past the 10s of centimeter scale [13]. Discretizing the lattice into building blocks which can then be assembled into arbitrarily large structures can leverage the benefits of cellular materials at larger size scales [1].

This work focuses on methods for automating the assembly of cellular materials at large scales using a voxelized approach. In prior work that demonstrated discrete cellular material for mid- to large- scale assemblies, such as for soft robotic [14], automotive [15], or aerospace [16] applications, the assemblies were composed manually— limiting the utility of these systems for broader application. Introducing a robotic assembly system would enable the adoption of the materials for wider use. To maintain global accuracy over the voxel structure, we adopted a relative robot approach to assembly [2], in which our robot and material systems are designed together, such that the material system is able to correct errors in the positioning of the robotic system. A prior robotic voxel assembly system, BILL-E [2], [9], [17] used a magnetic voxel feedstock with self-correcting features on the robot grippers to achieve consistent part placement in spite of the simplicity and minimal feedback present in the system. Similarly, brick- based systems, such as TERMES [5], a termite-inspired swarm construction system, or VaultBot [7], have also used specially designed bricks, both with magnetic insets, which interface with the assembly robot in specific ways to improve assembly performance.

Much of the prior work in modular robotics has also been concerned with developing modules that are able to be reconfigured in repeatable ways by an imprecise assembler— the modular robot itself. Robot modules typically have well-defined attachment points, leading toward chain- like geometries, in which modules attach end to end such as in [18], or grid-like geometries, in which modules can attach on multiple faces, such as in [19], though some work has also explored module attachment at arbitrary locations, such as [20]. These systems have employed a variety of attachment processes, such as motor-driven latching, as in [21] or [22], or phase change systems, such as through reflowing solder in [23], or melting a polymer [20]. The modular version of BILL- E [9] that this work extends on used a magnetic joint for the robot modules, which resulted in a low-strength connection that prevented the self-reproduction of that system and thus recursive assembly. Similarly, since the prior system only worked with magnetically connected voxel feedstock, the resulting structures could not bear load. The primary contribution of this paper is to demonstrate in hardware a modular robotic assembly system that is able to both assemble structures with desirable mechanical performance, and to assemble further robots.

III. ROBOT HARDWARE

A. Functional Voxels

The basis of the robotic system is a functional voxel— a building block element containing electronic functionality. [9] and [24] use a functional voxel made from PCB laminated to acetal, which uses soldered finger joints for the internal face connections and a combination of spring connectors and magnets for the voxel-to-voxel connections. For greater strength in that system, the magnets may be swapped for e.g. rivets, as done in [24], which renders the system more difficult to assemble robotically or to reconfigure. This work extends on the previously introduced design in [9] to incorporate a more mechanically stable joint compatible with robotic assembly, an increase in the amount of signals routed, and, optionally, the direct incorporation of microcontrollers into the voxel frame.

The functional voxel used here consists of six FR4 PCB faces assembled into a cuboctahedron or "cuboct" geometry. Similar to the work in [9], the joints within a voxel are epoxied and soldered. To enable autonomous connections between voxels without introducing significant additional weight, the system uses a reversible solder joint, modeled off of the system used in SolderCubes [23]. Like that system, the voxel faces have exposed pads primed with a low melt solder, and are heated using large surface mount resistors on the opposite side of the PCB. Unlike [23], we only use resistors on one side of the connection to reduce the amount of necessary electronic components, though it results in a longer attachment time— approximately six minutes to reliably flow and then cool the solder joint.

This system uses three main types of functional voxel faces. The first is a basic frame, which routes four signals— ground, supply voltage, serial clock, and serial data— and carries no additional electronic components. We then use two types of microcontroller faces: a primary controller face and a generic robot module face. The primary controller of the robot uses an ESP32-WROOM microcontroller, receiving commands over Wi-Fi from a central computer and disseminating these to the microcontrollers on each robot module over an I2C bus. The robot modules use ATtiny412 microcontrollers, which receive commands over the data lines and can either move a servo, report a measured joint angle, or activate the resistive heating circuit.

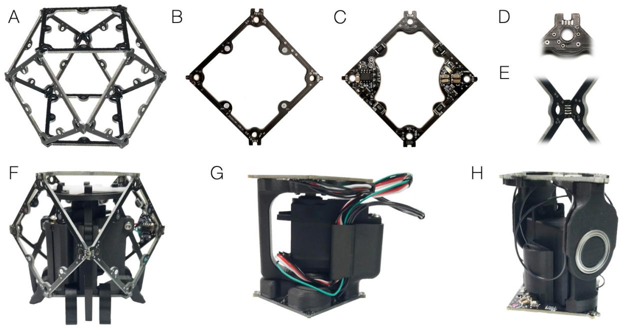

Fig. 2. Functional voxels and robot modules. A) A fully assembled functional voxel comprised of six PCB faces. B) The basic frame face, which routes four lines and carries no components. C) The ATtiny412 face, which controls the motor in each module. D) A close up view of the inner-voxel solder joint of one face. E) A close up view of a soldered inner-voxel joint. F) The gripper module. G) The wrist module. H) The elbow module.

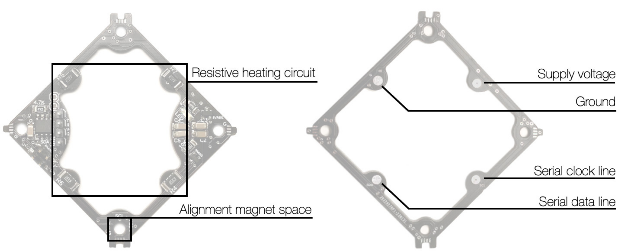

Fig. 3. Labeled components of two of the functional voxel frame types. (Left) ATtiny412 face with resistive heating circuit and alignment magnet install locations demarcated. (Right) Basic frame with the reflow solder signal pads labeled.

B. Modular Robot

Using this set of faces, we can build robotic modules by adding actuation. The robotic assembler makes use of three types of modules: a gripper, a wrist-type joint, and an elbow- type joint. The gripper attaches to voxels, enabling the robot to locomote over the lattice or to manipulate voxels. The wrist and elbow modules are both rotational joints with approximately 180 ° range of motion. To select an appropriate motor for the modules, we considered the potential worst case loading scenario— in which the robot cantilevers its entire length while carrying an additional module— and calculated the approximate required motor mass and stall torque required. Based on this, the FEETECH High-Torque Servo FS5115M-FB from Pololu was selected as a low cost and convenient option for the wrists and elbows with the feedback line broken out. The grippers use the smaller FEETECH Mini Servo FT1117M-FB from Pololu as the torque requirements are lower. The modules use FDM 3D printed parts to interface between the functional voxel faces and the motors. Parts were printed in either PLA (for the configuration 1 style robot, as shown in Fig. 4) or nylon with chopped carbon fiber (for the configuration 2 robot).

Modules are assembled into robots by stacking. The wrist and elbow type modules only accept connections from opposing ends (as in a chain-type modular robot), while the grippers can be configured to accept connections from any of the faces aside from the gripping surface. Though the robots explored in this project only make one connection from the grippers, future versions of the robot could add additional features by expanding from the grippers. Specifically, a separate gripping arm (as in [9]) could be added to improve the payload carrying ability of the robot. This paper explores two configurations of 6DoF robot, both of which use two grippers, two wrists, and four elbows. These configurations are shown in Fig. 4— in the first, there is an elbow joint immediately above the grippers, and then a wrist joint, while in the second the wrist joint comes first. The configuration 1 robot has a longer vertical reach than the configuration 2 robot, while the configuration 2 robot has a wider set of diagonal movement available to it.

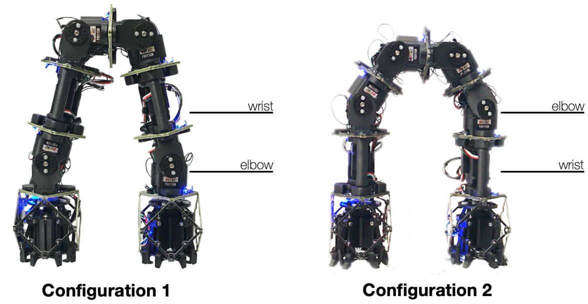

Fig. 4. Two configurations of robot that we explored. The different configurations have different accessible spaces, and so are better suited for different types of movement from each other.

IV. Construction Voxels

We used a face connected cuboctahedron unit cell, as done in [13]. The unit cell is decomposed into six 2D faces which are snap-fit assembled together and then decorated with latching features to facilitate voxel-to-voxel connections. Voxels are designed to be installed and removed vertically, for ease of robotic assembly. Because the voxel design is based on 2D faces, it is compatible with a range of materials. For this work, we primarily used aluminum voxels or acetal voxels. The aluminum voxels were made either from laser cut aluminum or were purchased as aluminum PCBs from JLCPCB. PCB manufacturing was chosen as it is a cheap process— individual faces were priced at less than 0.30USD per face at 250 order quantity. Acetal voxels were laser cut.

Two clip families were used. In the first, the clips constrain all but one degree of freedom once a voxel is placed, and require the installation of an additional clip to fully constrain the voxel. In the second, the clips are designed with snap fit features, such that once placed, the voxel is fully constrained. A variety of vertical clip types were explored, though all utilized snap fit features to attach to the lower voxel.

The voxels were mechanically characterized through Instron testing. We primarily used acetal voxels for the testing to characterize the behavior of the joint and voxel geometry.

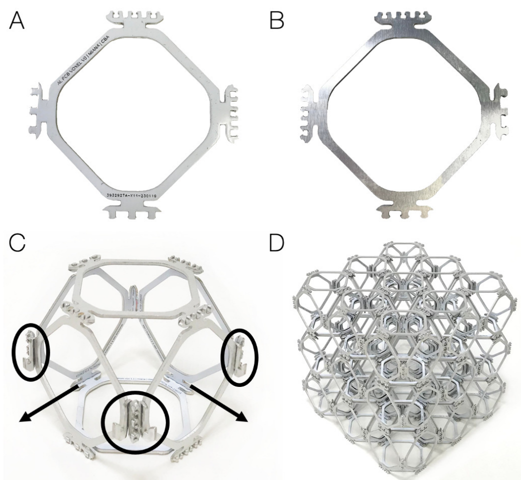

Fig. 5. The construction voxel system. A) A single aluminum PCB voxel face from the top view. B) The bottom view of the same voxel face. C) A voxel with the lateral connection clips highlighted and the assembly direction demarcated. D) A 3x3x3 assembly of voxels for characterizing the behavior of the bulk material.

Fig. 6. Some clips explored for this system. (Clockwise, from top left corner) A vertical connector clip, another variant of the vertical connector clip, a snap fit lateral joint, a smaller snap fit lateral joint, a shear clip, a small press-fit joint, a larger press-fit joint, another variant of vertical clip, and yet another variant of the vertical clip.

For this, we tested 1- and 2- voxel stacks under tension and compression, with fixtures matching how loads would be applied to a voxel in a lattice. We tested the joints under tension, in shear, and under cyclic loading. We additionally tested the aluminum voxels under compression to examine the bulk material behavior and scaling. Some of the key results from this testing are summarized in Table 1. Specifically, the modulus (MPa) and load (N) are reported for 1- and 2- acetal voxel assemblies tested in compression and tension (each of these tests is repeated three times), as well as for acetal and aluminum 2x2x2 and 3x3x3 voxel assemblies (which are only tested once). For complete testing results, see [25].

The immediate goal of the construction voxels is to provide a lightweight load bearing system— which the current design succeeds at— with a secondary goal of achieving behavior equivalent to a continuously manufactured cuboctahedron lattice— which the current design falls short of. The 3x3x3 aluminum structure has a density of 62.5 Kg/m^3, a compressive modulus of 5.1 MPa, and reached a maximum load of 4576.68 N, placing the lattice's mechanical behavior in a similar range to some metal lattices in [26], or the plastic and composite lattices in [12] or [13].

TABLE I

Summarized Voxel Mechanical Properties

Part	Material	Test	Modulus (MPa)	Max. load (N)
1x1x1	acetal	C	0.404 ± 0.009	137.29 ± 1.45
1x1x1	acetal	T	0.367 ± 0.012	210.56 ± 22.22
2x1x1	acetal	C	0.372 ± 0.003	134.52 ± 0.46
2x1x1	acetal	T	0.314 ± 0.009	82.55 ± 26.52
2x2x2	acetal	C	0.518	513.30
3x3x3	acetal	C	0.522	1055.14
1x1x1	aluminum	C	4.50	353.27
2x2x2	aluminum	C	5.07	2028.4
3x3x3	aluminum	C	5.10	4576.68

However, for this lattice geometry, we would expect better performance, as well as a larger improvement in the modulus as the voxel count increases, as reported for the systems described in [27] or [13]. To reach this ideal behavior, the behavior of the voxel structure needs to be dominated by the behavior of the beams, as opposed to the joints. Because of the current design of the clips and interfacing features in the voxels, this is not achieved. A single acetal voxel in tension reaches a maximum load of 210.56 ± 22.22 N, while two acetal voxels in tension (which now have clips between them), only reach a maximum load of 82.55 ± 26.52 N before failure, clearly indicating that the clips are a weak point in the system. Similarly, the variance in the maximum loads reached in compressive tests is much lower than that of the tensile tests, indicating that the clips behave less consistently than the voxels. The indexing features on the voxel faces, as well as the clips themselves, introduce additional compliance in the system that prevents optimal behavior.

V. Controls and Simulation

We developed a custom web-based design and simulation tool to be able to test different control and path planning strategies for the assemblers, as well as further explore different robot designs and architectures. Fig. 7 shows an interactive interface that does the inverse kinematics for the robot given a target end position.

We implement the centralized path planning algorithm and the shape compiler introduced in [2]. The algorithm calculates the steps needed to build an arbitrary geometry given one or multiple voxel deposit locations. These steps are later sent to the physical robots to start assembling the structure. Using this algorithm, the robot can build any connected geometry that does not have underhangs, layer by layer. It is possible for horizontal layers to have unconnected areas, as long as all voxels are connected to voxels in the layer beneath them. We also implemented the spatio-temporal scheduling scheme introduced in [2] to do path planning for multiple robots. Fig. 8 shows an example of two robots collaborating to build a spanning structure.

Fig. 9 shows some robot design explorations using the simulation tool. Using the set of modules that we introduced, one can design robots that are able to carry a larger number of voxels, or collaborate to carry out harder tasks that cannot be achieved by a single robot. The custom design tool makes it easier to explore and simulate these variations in an easy parametric manner.

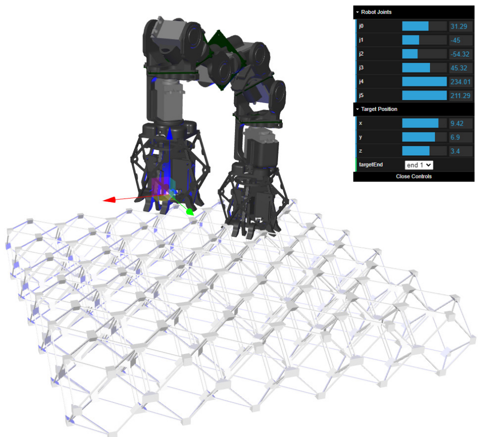

Fig. 7. Screenshot of the inverse kinematics web interface. The robot end effector position may be changed by dragging the axis, or by toggling the joint position.

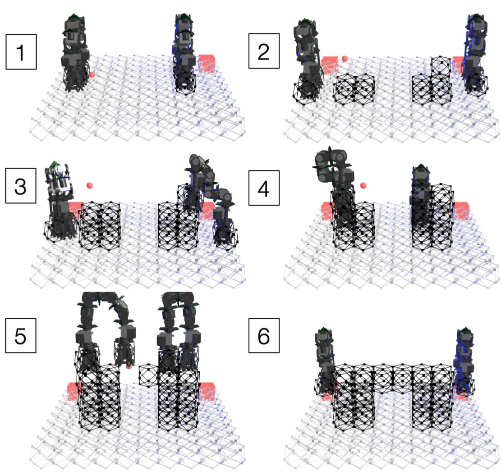

Fig. 8. Stills from the path planning tool of two robots assembling a spanning structure.

VI. ROBOTIC ASSEMBLY SYSTEM

A. Assembly demonstrations

The robotic system was primarily evaluated through demonstrations of fundamental assembly tasks— the construction of a 1D beam, a 2D cube, and another robot. We used the robots to build beams and small cubes (2x2x2 voxels) out of aluminum voxels. Fig. 10 shows the basic steps for voxel assembly. The robot starts standing on the build plate and a new voxel is manually fed in. The robot swings around to pick up the new voxel, grabs it, and places it. If using the snap-fit clips, then this placement is stable, otherwise, an additional clip is required. A new voxel is then fed in.

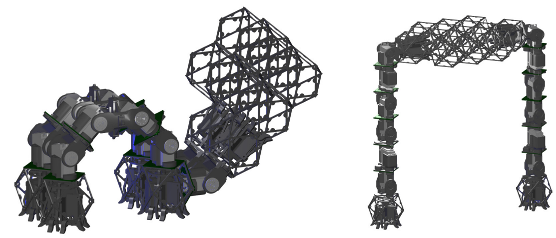

Fig. 9. Renderings of notional alternate robot geometries with larger payload carrying abilities from the design tool. (Left) a parallelized version of the current assembler, shown carrying 8 voxels. (Right) Two of the current robot configurations holding 9 voxels together, acting temporarily as one larger robot.

This basic sequence is also used for assembling additional robots. New robot modules are fed into the manual feed location. After the placement of the first module, which must contain the second robot's ESP32 primary controller, power is wired to the second module. The first robot can then stack modules to build out the robot, with the second robot running its resistive heating routine after the placement of each new voxel. Magnets installed in the faces of the modules, as well as some extending 3D features in the modules, help with consistent module alignment, in spite of imprecision from the assembling robot.

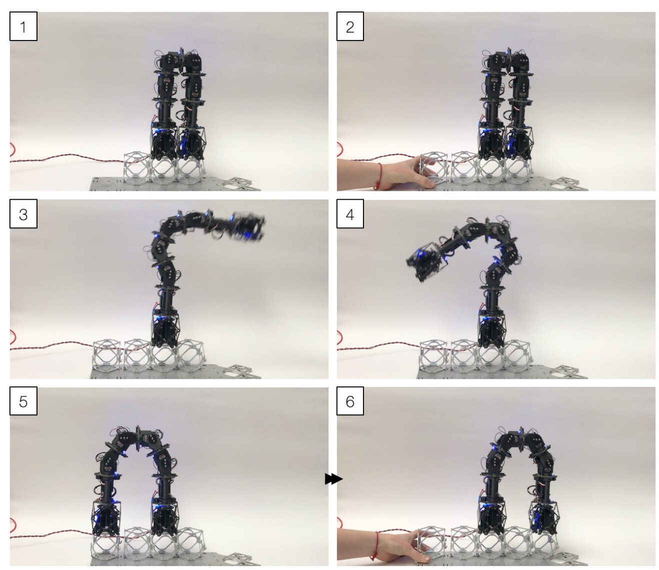

Fig. 10. The basic assembly sequence. 1) The robot starts standing on the build plate. 2) A voxel is manually fed in. 3-5) The robot swings back to grab the voxel. 6) The robot places the voxel and a new voxel is fed in.

At a certain point, the assembling robot is no longer able to reach the next module placement for the robot it is assembling. At this point, the assembled robot can help the assembling robot by moving to accessible positions, as shown in Fig. 11. Fig. 11 shows this assembly sequence for the attachment of the last two modules. The robot that is being assembled moves itself so that the assembling robot can reach the next placement location, and then moves out of the way, so that the assembling robot can pick up the next module. This is continued until the second robot is complete.

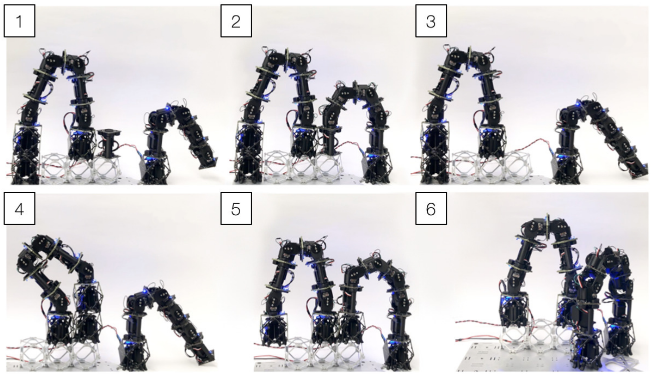

Fig. 11. A portion of the robotic assembly of a second robot. 1) The 7th module of the assembled robot is placed on the lattice. 2-3) the assembled robot connects to it, and 4) the assembler places the last module. 5-6) The last module is connected to form two robots.

Once there are two robots, the robots may collaborate with each other to improve the overall performance of the system. We demonstrate a basic version of this collaboration by having both robots work on the assembly of a four voxel cantilever beam that supports the weight of the assembly robot (see Fig. 12 for reference). The robots initially build out a 3-voxel beam from the build platform, as done in Fig. 10, and then they add another 2 voxels on top of that beam, allowing the second robot to step up onto the initial cantilever. From there, the first robot picks up and passes voxels to the second one, which then places those voxels to extend the cantilever.

As is visible in Fig. 12, the beam does visibly deflect under the weight of the robot, which would negatively impact the ability of the system to continue accurately building out the beam for a different geometry (e.g., if the beam were built to bridge between two voxel structures, the deflection could potentially prevent the accurate indexing of the voxels onto the other side). Currently, the path-planning systems do not account for this type of non-ideal behavior. Future work will address this by iterating the material system to make it stiffer, as well as potentially advancing the path planning software to account for local material deformations during assembly.

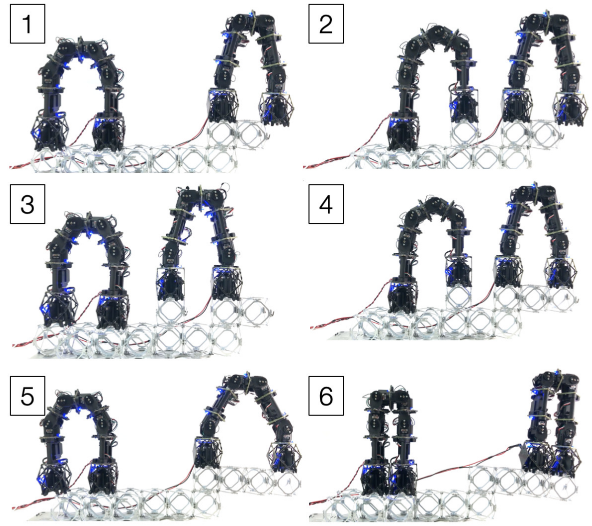

Fig. 12. Collaborative robotic assembly of a cantilever beam that supports the weight of one robot. 1) Robot 1 picks up a voxel and 2) passes it to robot 2. 3) Robot 1 returns to the voxel feed location, while robot 2 grabs the voxel left by robot 1. 4) While robot 1 delivers the next voxel to robot 2, robot 2 extends the cantilever. 5) Robot 1 reverts to its initial position and robot 2 builds out the cantilever. 6) Robot 2 walks to the end of the cantilever beam.

VII. Discussion

The robotic assembly system demonstrates in hardware the basic functionality for a self-reproducing assembly swarm: the robot can make another robot, and these robots can build load bearing structures, advancing it past the prior BILL-E assemblers this work extends on. This work is a starting point for this system, though, and so still faces challenges before it can fully realize the goal of an autonomously self-scaling swarm construction system.

The relative robot building strategy assumes that the interface between the robot and the material is reliable enough to correct any failures in the positioning of the robot. To evaluate this assumption, the repeatability of this system was tested by repeatedly walking the robot back and forth on a voxel structure. Specifically, the configuration 2 style robot walked back and forth over a voxel beam, using three different step types. The overall failure rate was 7.1 %. These failures occured primarily because the robot could not detect if a step failed— further iteration of the gripping leg flexure design would help mitigate failures, while the addition of a minimal feedback system, such as the switch used in [17], could allow the robot to self-correct.

Because the robot does not have additional voxel carrying capabilities, to build beyond its reach, it must place voxels in temporary locations, and then pick and place them to their final location. This is less efficient than simply carrying the voxels, and introduces more steps during which the robot could fail. We will likely add a third gripper to the robot, as done in [9] to resolve this.

We only demonstrate collaborative robotic behavior in a limited manner. Even though for a structure with this few voxels, the use of two robots does not substantially improve the time efficiency of the system, this represents a small-scale demonstration of the type of collaborative robotic behavior we want to further develop, such that it enables the efficient assembly of eventually large structures. The current system does not use online planning, that is, path planning is done on a central computer and exported to the robots that then execute, analogous to running g-codes on CNC machines. Future work could explore online planning algorithms, such as those described in [28], and work up towards replicating in hardware the results described in [9], specifically in exploring hierarchical robot configurations.

REFERENCES

[1] K. C. Cheung and N. Gershenfeld, "Reversibly Assembled Cellular Composite Materials," Science, vol. 341, no. 6151, pp. 1219-1221, Sep. 2013, doi: 10.1126/science.1240889.

[2] B. Jenett, A. Abdel-Rahman, K. Cheung, and N. Gershenfeld, "Material-Robot System for Assembly of Discrete Cellular Structures," IEEE Robot. Autom. Lett., vol. 4, no. 4, pp. 4019-4026, Oct. 2019, doi: 10.1109/LRA.2019.2930486.

[3] A. Mirjan, F. Augugliaro, R. D'Andrea, F. Gramazio, and M. Kohler, "Building a Bridge with Flying Robots," in Robotic Fabrication in Architecture, Art and Design 2016, D. Reinhardt, R. Saunders, and J. Burry, Eds., Cham: Springer International Publishing, 2016, pp. 34-47.

[4] V. Helm, J. Willmann, F. Gramazio, and M. Kohler, "In-Situ Robotic Fabrication: Advanced Digital Manufacturing Beyond the Laboratory," in Gearing Up and Accelerating Cross-fertilization between Academic and Industrial Robotics Research in Europe:, F. Röhrbein, G. Veiga, and C. Natale, Eds., in Springer Tracts in Advanced Robotics. Cham: Springer International Publishing, 2014, pp. 63-83.

[5] "Designing Collective Behavior in a Termite-Inspired Robot Construction Team." https://www.science.org/doi/10.1126/science.1245842 (accessed Sep. 15, 2023).

[6] S. Leder et al., "Leveraging Building Material as Part of the In-Plane Robotic Kinematic System for Collective Construction," Adv. Sci., vol. 9, no. 24, p. 2201524, 2022, doi: 10.1002/advs.202201524.

[7] N. Melenbrink, A. Wang, and J. Werfel, "An Autonomous Vault-Building Robot System for Creating Spanning Structures," in 2021 IEEE International Conference on Robotics and Automation (ICRA), May 2021, pp. 7066–7072. doi: 10.1109/ICRA48506.2021.9561004.

[8] A. Hsu et al., "Application of micro-robots for building carbon fiber trusses," in 2016 International Conference on Manipulation, Automation and Robotics at Small Scales (MARSS), Jul. 2016, pp. 1–6. doi: 10.1109/MARSS.2016.7561729.

[9] A. Abdel-Rahman, C. Cameron, B. Jenett, M. Smith, and N. Gershenfeld, "Self-replicating hierarchical modular robotic swarms," Commun. Eng., vol. 1, no. 1, p. 35, Nov. 2022, doi: 10.1038/s44172-022-00034-3.

[10] T. A. Schaedler, A. Jacobsen, A. Torrents, A. Sorensen, J. Lian J. Greer, L. Valdevit, and W. Carter. (2011). Ultralight Metallic Microlattices. Science (New York, N.Y.). 334. 962-5. 10.1126/science.1211649.

[11] T. A. Schaedler and W. B. Carter, "Architected Cellular Materials," Annu. Rev. Mater. Res., vol. 46, no. 1, pp. 187–210, 2016, doi: 10.1146/annurev-matsci-070115-031624.

[12] X. Zheng et al., "Ultralight, ultrastiff mechanical metamaterials," Science, vol. 344, no. 6190, pp. 1373–1377, Jun. 2014, doi: 10.1126/science.1252291.

[13] B. Jenett, C. Cameron, F. Tourlomousis, A. P. Rubio, M. Ochalek, and N. Gershenfeld, "Discretely assembled mechanical metamaterials," Sci. Adv., vol. 6, no. 47, p. eabc9943, Nov. 2020, doi: 10.1126/sciadv.abc9943.

[14] A. Parra Rubio et al., "Modular Morphing Lattices for Large-Scale Underwater Continuum Robotic Structures," Soft Robot., vol. 10, no. 4, pp. 724–736, Aug. 2023, doi: 10.1089/soro.2022.0117.

[15] B. E. Jenett, "Discrete mechanical metamaterials," Thesis, Massachusetts Institute of Technology, 2020. Accessed: Sep. 15, 2023. [Online]. Available: https://dspace.mit.edu/handle/1721.1/130610

[16] B. Jenett et al., "Digital Morphing Wing: Active Wing Shaping Concept Using Composite Lattice-Based Cellular Structures," Soft Robot., vol. 4, no. 1, pp. 33–48, Mar. 2017, doi: 10.1089/soro.2016.0032.

[17] B. Jenett and K. Cheung, "BILL-E: Robotic Platform for Locomotion and Manipulation of Lightweight Space Structures," in 25th AIAA/AHS Adaptive Structures Conference, Grapevine, Texas: American Institute of Aeronautics and Astronautics, Jan. 2017. doi: 10.2514/6.2017-1876.

[18] M. Yim, D. G. Duff, and K. D. Roufas, "PolyBot: a modular reconfigurable robot," in Proceedings 2000 ICRA. Millennium Conference. IEEE International Conference on Robotics and Automation. Symposia Proceedings (Cat. No.00CH37065), Apr. 2000, pp. 514–520 vol.1. doi: 10.1109/ROBOT.2000.844106.

[19] A. Spröwitz, R. Moeckel, M. Vespignani, S. Bonardi, and A. J. Ijspeert, "Roombots: A hardware perspective on 3D self-reconfiguration and locomotion with a homogeneous modular robot," Robot. Auton. Syst., vol. 62, no. 7, pp. 1016–1033, Jul. 2014, doi: 10.1016/j.robot.2013.08.011.

[20] P. Swissler and M. Rubenstein, "FireAnt3D: a 3D self-climbing robot towards non-latticed robotic self-assembly," in 2020 IEEE/RSJ International Conference on Intelligent Robots and Systems (IROS), Las Vegas, NV, USA: IEEE, Oct. 2020, pp. 3340–3347. doi: 10.1109/IROS45743.2020.9341116.

[21] H. Kurokawa, K. Tomita, A. Kamimura, S. Kokaji, T. Hasuo, and S. Murata, "Distributed Self-Reconfiguration of M-TRAN III Modular Robotic System," Int. J. Robot. Res., vol. 27, no. 3–4, pp. 373–386, Mar. 2008, doi: 10.1177/0278364907085560.

[22] C. H. Belke and J. Paik, "Mori: A Modular Origami Robot," IEEEASME Trans. Mechatron., vol. 22, no. 5, pp. 2153–2164, Oct. 2017, doi: 10.1109/TMECH.2017.2697310.

[23] J. Neubert and H. Lipson, "Soldercubes: a self-soldering self-reconfiguring modular robot system," Auton. Robots, vol. 40, no. 1, pp. 139–158, Jan. 2016, doi: 10.1007/s10514-015-9441-4.

[24] C. G. Cameron, Z. Fredin, and N. Gershenfeld, "Discrete Assembly of Unmanned Aerial Systems," in 2022 International Conference on Unmanned Aircraft Systems (ICUAS), Dubrovnik, Croatia: IEEE, Jun. 2022, pp. 339–344. doi: 10.1109/ICUAS54217.2022.9836082.

[25] M. M. Smith, "Recursive Robotic Assemblers," Thesis, Massachusetts Institute of Technology, 2023. Accessed: Sep. 14, 2023. [Online]. Available: https://dspace.mit.edu/handle/1721.1/152015

[26] B. Jenett, N. Gershenfeld, and P. Guerrier, "Building Block-Based Assembly of Scalable Metallic Lattices," in Volume 4: Processes, College Station, Texas, USA: American Society of Mechanical Engineers, Jun. 2018, p. V004T03A053. doi: 10.1115/MSEC2018-6442.

[27] C. E. Gregg, J. H. Kim, and K. C. Cheung, “Ultra-Light and Scalable Composite Lattice Materials,” Adv. Eng. Mater., vol. 20, no. 9, p. 1800213, 2018, doi: 10.1002/adem.201800213.

[28] A. Costa, A. Abdel-Rahman, B. Jenett, N. Gershenfeld, I. Kostitsyna, and K. Cheung, “Algorithmic Approaches to Reconfigurable Assembly Systems,” in 2019 IEEE Aerospace Conference, Big Sky, MT, USA: IEEE, Mar. 2019, pp. 1–8. doi: 10.1109/AERO.2019.8741572.